THE JOURNAL OF BIOLOGICAL CHEMISTRY VOL. 286, NO. 7, pp. 5647–5656, February 18, 2011


# Munc13-4 Restricts Motility of Rab27a-expressing Vesicles to Facilitate Lipopolysaccharide-induced Priming of Exocytosis in Neutrophils*[S]

Received for publication, September 17, 2010, and in revised form, December 7, 2010 Published, JBC Papers in Press, December 9, 2010, DOI 10.1074/jbc.M110.184762

**Jennifer L. Johnson[‡], Hong Hong[‡], Jlenia Monfregola[‡], William B. Kiosses[§], and Sergio D. Catz[‡1]**

*From the [‡]Department of Molecular and Experimental Medicine and [§]Core Microscopy Facility, The Scripps Research Institute, La Jolla, California 92037*

**LPS is an efficient sensitizer of the neutrophil exocytic response to a second stimulus. Although neutrophil exocytosis in response to pathogen-derived molecules plays an important role in the innate immune response to infections, the molecular mechanism underlying LPS-dependent regulation of neutrophil exocytosis is currently unknown. The small GTPase Rab27a and its effector Munc13-4 regulate exocytosis in hematopoietic cells. Whether Rab27a and Munc13-4 modulate discrete steps or the same steps during exocytosis also remains unknown. Here, using Munc13-4- and Rab27a-deficient neutrophils, we analyzed the mechanism of lipopolysaccharide-dependent vesicular priming to amplify exocytosis of azurophilic granules. We found that both Munc13-4 and Rab27a are necessary to mediate LPS-dependent priming of exocytosis. However, we show that LPS-induced mobilization of a small population of readily releasable vesicles is a Munc13-4-dependent but Rab27a-independent process. LPS-induced priming regulation could not be fully explained by secretory organelle maturation as the redistribution of the secretory proteins Rab27a or Munc13-4 in response to LPS treatment was minimal. Using total internal reflection fluorescence microscopy and a novel mouse model expressing EGFP-Rab27a under the endogenous Rab27a promoter but lacking Munc13-4, we demonstrate that Munc13-4 is essential for the mechanism of LPS-dependent exocytosis in neutrophils and unraveled a novel mechanism of vesicular dynamics in which Munc13-4 restricts motility of Rab27a-expressing vesicles to facilitate lipopolysaccharide-induced priming of exocytosis.**

Neutrophil exocytosis in response to pathogen-derived molecules plays an important role in extracellular bacterial killing and response to infection (1, 2). The Gram-negative bacterial cell wall component LPS is a relatively weak agonist for neutrophil exocytosis but is an efficient sensitizer of the neutrophil exocytic response to a second stimulus (3), a mechanism usually referred to as "priming" (4). The amplification of the neutrophil secretory process by LPS plays a very important role during the neutrophil response to Gram-negative bacterial infections, in which neutrophils are exposed to multiple pathogen-associated molecular patterns and to endogenous inflammatory cytokines (5, 6). Although the molecular mechanisms that mediate LPS-induced neutrophil priming and the molecular components involved in LPS-induced exocytosis of azurophilic granules are currently unknown, our previous studies showing that mice deficient for the small GTPase Rab27a have impaired secretion of myeloperoxidase (MPO)[2] in response to LPS *in vivo* suggest that Rab27a plays a significant role in this process (7).

Rab27a and Munc13-4 are master regulators of exocytosis in hematopoietic cells. Genetic defects in the *Rab27a* or *Unc13D* gene lead to the human immunodeficiencies Griscelli syndrome type 2 and familial hemophagocytic lymphohistiocytosis 3, respectively (8, 9). Munc13-4 is a 120-kDa protein, which coordinates vesicular trafficking and exocytosis in many cellular systems (3, 9–11). Previous studies have demonstrated that Munc13-4 is essential for lytic granule exocytosis at the immunological synapse (9), neutrophil granule secretion (3), and platelet-dense granule exocytosis (11). Based on pulldown studies and molecular interaction assays, it was proposed that Munc13-4 is a specific effector of the small GTPase Rab27a (11, 12), which also plays an important role in the regulation of secretory lysosome exocytosis (13). Despite shared roles in regulating common secretory pathways, it is unclear whether they act together to regulate the same steps during exocytosis. In this way, several lines of evidence suggest that Rab27a and Munc13-4 regulate discrete molecular events during secretory lysosome exocytosis (14, 15). Other studies suggest a possible combined role for Munc13-4 and Rab27a during lytic granule maturation (16). In neutrophils, both Rab27a and Munc13-4 regulate the exocytosis of secretory organelles (3, 7, 17), although whether they jointly or independently regulate transport toward the plasma membrane (PM), tethering, docking, or fusion is currently unknown and needs further characterization.

Most of our current understanding of the mechanism of secretory lysosome exocytosis is based on static observations, *i.e.* microscopic observations of the distribution of granule components before and after stimulation. These experiments

* This work was supported, in whole or in part, by National Institutes of Health Grant HL088256 from the U. S. Public Health Service (to S. D. C.).

[S] The on-line version of this article (available at http://www.jbc.org) contains supplemental Figs. S1 and S2 and Movies 1–4.

[1] To whom correspondence should be addressed: Dept. of Molecular and Experimental Medicine, The Scripps Research Institute, 10550 N. Torrey Pines Rd., La Jolla, CA 92037. Tel.: 858-784-7932; Fax: 858-784-2054; E-mail: scatz@scripps.edu.

[2] The abbreviations used are: MPO, myeloperoxidase; PM, plasma membrane; TIRFM, total internal reflection fluorescence microscopy; EGFP, enhanced GFP; fMLF, formyl-methionyl-leucyl-phenylalanine.

have contributed invaluable information to our current understanding of the mechanism under study; however, secretory vesicles are highly dynamic before exocytosis (3, 18), and putative changes in vesicular dynamics during the priming and/or maturation process of secretory organelles in hematopoietic cells are poorly understood. In this work, we took a live-cell microscopic approach to study the dynamic mechanisms of granule priming and exocytosis. To test the hypothesis that Munc13-4 and Rab27a control a common secretory pathway, we generated a unique animal model consisting of a mouse chimera obtained by crossing Munc13-4-deficient mice (*Jinx*) with *EGFP-Rab27a* transgenic mice expressing EGFP-Rab27a under the endogenous Rab27a promoter ($Tg^{EGFP\text{-}Rab27a}$). Using neutrophils as a model, we performed vesicle dynamics studies to unravel a novel regulatory role of Munc13-4 and Rab27a in lipopolysaccharide-induced granule priming and exocytosis in hematopoietic cells.

## EXPERIMENTAL PROCEDURES

*Experimental Animal Models*—Our experiments utilize *Jinx* mice (C57BL/6-Munc13-$4^{Jinx/Jinx}$) (19), *ashen* mice (C57BL/6-$Rab27a^{ash/ash}$) (20), and their parental strain C57BL/6(BL6). The Munc13-4-deficient mouse model Jinx was generated by random germ line mutagenesis using the alkylating agent *N*-ethyl-*N*-nitrosourea (19). Munc13-$4^{Jinx/Jinx}$ was maintained as a homozygous stock for use in these studies. $Rab27a^{ash/ash}$ mice that contain a splicing mutation in the *Rab27a* gene have been extensively utilized for the study of Rab27a deficiency and were described previously (20). C57BL/6J control mice were obtained from the animal resource center at The Scripps Research Institute.

Our experiments utilize a novel animal model generated by crossing Munc13-$4^{Jinx/Jinx}$ mice with FR84 EGFP-Rab27a transgenic mouse ($Tg^{EGFP\text{-}Rab27a}$), which expresses EGFP-Rab27a under the control of endogenous *Rab27a* promoter and subsequently crossing the heterozygous progeny. $Tg^{EGFP\text{-}Rab27a}$-Munc13-$4^{Jinx/Jinx}$ were genotyped using tail-extracted genomic DNA as follows. The genotyping reactions for EGFP-Rab27a transgenic mouse utilized the forward primer 5′-AGGTTTCGTAGCTTAACGACAGCGTTCTTC and the reverse primer 5′-ATAAGAGTCTCTTCTGTGGG to amplify a 385-bp fragment, using a polymerase chain reaction as described previously (21). The genotyping reactions for Munc13-$4^{Jinx/Jinx}$ used the forward primer 5′-CTACATGAACACCAACCTGGTCCAGGAG-3′ and the reverse primer 5′-GATCATGAAGAGGAAGGAGATGCAGTTAGG-3′ in PCR reactions as described (19). PCR reactions were subsequently sequenced using the following sequencing primer, 5′-TACATGAACACCAACCTGGTCC-3′, also as described (19).

$Tg^{EGFP\text{-}Rab27a}$ transgenic mice are extensively characterized, are fully functional and rescued the two major defects of the *ashen* Rab27a knock-out mouse (21). Furthermore, cell-specific expression of EGFP-Rab27a in FR84 EGFP-Rab27a transgenic mouse faithfully followed the pattern of expression of endogenous Rab27a (21). All studies were performed using 6–8-week old mice and conducted according to the National Institutes of Health and institutional guidelines and with approval of the institutional animal review board.

*Neutrophil Functional Assays*—Peripheral murine neutrophils were obtained from blood collected by cardiac puncture, and erythrocytes were removed by lysis using a solution consisting of 168 mM $NH_4Cl$, 10 mM Tris/HCl, pH 7.4. Neutrophils were isolated using MACS® technology with anti-mouse Ly-6G (clone 1A8) biotin, anti-biotin microbeads, and MS MACS columns, as described by the manufacturer (Miltenyi Biotec). The cells were washed once with 1% BSA in PBS and kept in ice until used. Bone marrow-derived neutrophils were isolated using a Percoll-gradient fractionation system, and neutrophil secretion studies were performed as described previously (22). The analysis of secreted and total cell lysate myeloperoxidase was performed using a murine MPO-specific enzyme-linked immunosorbent assay (HyCult Biotechnology) according to the manufacturer's instructions.

*TIRF Microscopy and Data Analysis*—For live-cell total internal reflection fluorescence microscopy (TIRFM) imaging, neutrophils isolated from $Tg^{EGFP\text{-}Rab27a}$ transgenic mice or $Tg^{EGFP\text{-}Rab27a}$-Munc13-$4^{Jinx/Jinx}$ mice were resuspended in phenol red-free RPMI medium and transferred to eight-well plates with bottom coverglass (1.5 borosilicate coverglass, Lab-Tek, Nunc). The cells were incubated in the presence of serum-activated LPS (100 ng/ml) or medium for 2 h at 37 °C and rapidly transferred to a prewarmed microscope stage. TIRFM experiments were performed using a 100 × 1.45 numerical aperture TIRF objective (Nikon) on a Nikon TE2000U microscope custom modified with a TIRF illumination module. Laser illumination (488 laser line) was adjusted to impinge on the coverslip at an angle to yield a calculated evanescent field depth ($d$) < 100 nm. Images were acquired on a 14 bit, cooled charge-coupled device camera (Hamamatsu) controlled through NIS-Elements software (Nikon, Inc.). The images were recorded at 1-s intervals using exposure times of 200–600 ms, depending on the intensity of the signal. Images were analyzed using ImageJ (version 1.43) and IMARIS (version 7.0) software (Bitplane Scientific Software). All data analysis was performed by tracking granule movement through all frames of the movies. All vesicles that appeared in the TIRFM zone for at least three frames during the length of the study were included in the analysis. Images that experienced mild fading over time were autothresholded in IMARIS to ensure that regions of interest (vesicle center or centroid) were continually tracked throughout the period monitored.

For the analysis of the distribution of endogenous myeloperoxidase, neutrophils were transferred to chambered coverglass (Lab-Tek 1.5, Nunc), fixed with 3.7% paraformaldehyde, permeabilized with 0.01% saponin, and blocked with a solution of 1% BSA in PBS as described (22). Samples were labeled with anti-murine MPO-specific antibody (HyCult Biotec), anti-Munc13-4 antibodies (described previously in Ref. 3) or anti-EGFP monoclonal or polyclonal antibodies (Santa Cruz Biotechnology) overnight at 4 °C. Subsequently, the samples were incubated with Alexa Fluor 488- or 568-conjugated secondary antibodies (Molecular Probes). The cells were stored in unsolidified water-based mounting medium (refractive index, 1.37) until analyzed. TIRFM experiments

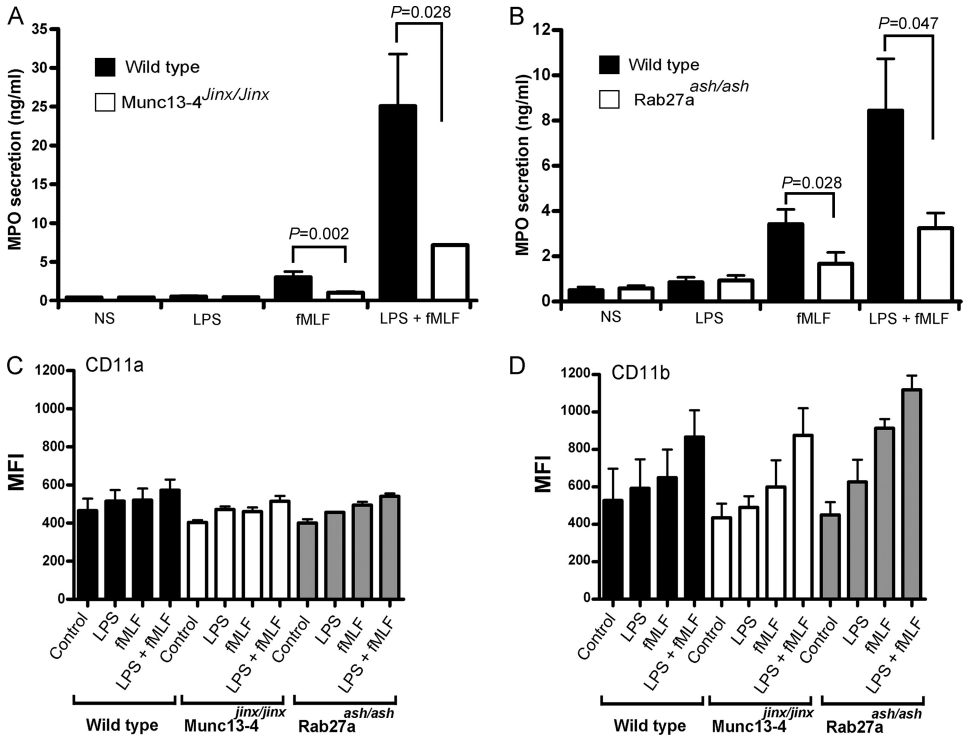


FIGURE 1. **Munc13-4 and Rab27a regulate LPS-dependent priming and exocytosis of azurophilic granules.** Wild type and Munc13-4$^{Jinx/Jinx}$ (*A*) or Rab27a$^{ash/ash}$ (*B*) neutrophils were stimulated with LPS (100 ng/ml) or fMLF (1 $\mu$M) or incubated for 30 min in the presence of LPS followed by a 30-min stimulation with fMLF. MPO release was measured by ELISA. *C* and *D*, neutrophils from wild type, *ashen*, or *Jinx* mice were stimulated with the indicated agonist or left untreated, and the plasma membrane expression of the adhesion molecules CD11a and CD11b was detected by flow cytometry. All results represent the mean ± S.E., and statistically significant differences were calculated using unpaired Student's *t* test ($n = 3–6$). *MFI*, mean fluorescence intensity; *NS*, unstimulated.

were performed as described above except that the images were recorded using 300–500 ms exposure times depending on the intensity of the signal. Images were analyzed using ImageJ software (version 1.43), and vesicles were quantified using Quantity One analysis software (Bio-Rad).

*Statistical Analysis*—Data are presented as means, and error bars correspond to S.E. Statistical significance was determined using unpaired Student's *t* test unless stated otherwise. Statistical analysis was performed using GraphPad InStat 3, and graphs were made using GraphPad Prism 4. Differences were considered statistically significant at $p < 0.05$.

## RESULTS

*Munc13-4 and Rab27a Are Essential Regulators of Neutrophil Exocytic Response to Lipopolysaccharide*—To analyze the role of Munc13-4 and Rab27a in LPS-dependent priming and exocytosis, we studied the exocytic response of Munc13-4-null (Munc13-4$^{Jinx/Jinx}$) and Rab27a-deficient (*ashen*, Rab27a$^{ash/ash}$) neutrophils to LPS *ex vivo*. First, we showed that murine neutrophils have a very weak exocytic response to LPS when used as a solo stimulus (Fig. 1*A*). Next, we analyzed the neutrophil secretory response to the bacteria-derived chemotactic peptide formyl-methionyl-leucyl-phenylalanine (fMLF), a well known stimulus of neutrophil secretion (3). Although neutrophils from wild type mice showed a significant but modest secretory response to fMLF, Munc13-4$^{Jinx/Jinx}$ neutrophils showed an impaired response to the chemotactic peptide (Fig. 1*A*). Importantly, the secretory response to fMLF increased significantly when wild type neutrophils were treated with LPS for 30 min prior to stimulation with the chemotactic peptide indicating that, similar to human neutrophils (3), mouse neutrophils are susceptible to LPS-dependent priming for exocytosis (Fig. 1*A*). Contrarily to that observed in wild type cells, azurophilic granule exocytosis was markedly impaired in neutrophils from Munc13-4$^{Jinx/Jinx}$ mice even after LPS-induced priming (Fig. 1*A*), suggesting that Munc13-4 is an important regulator of LPS-dependent neutrophil priming or may regulate a post-priming mechanism during azurophilic granule exocytosis.

To test the hypothesis that Munc13-4 and Rab27a control a common secretory pathway, we subsequently evaluated whether the secretory response of neutrophils from Rab27a-deficient mice was also impaired. Similar to that shown for Munc13-4-deficient mice, Rab27a$^{ash/ash}$ neutrophils showed a marked defect in their secretory response to the chemotactic peptide under both LPS-primed and unprimed conditions (Fig. 1*B*). The similar exocytic defects observed in Munc13-4- and Rab27a-deficient neutrophils suggested that both Munc13-4 and Rab27a are necessary for LPS-mediated priming of chemotactic peptide-induced azurophilic granule secretion in neutrophils and raised the question of whether Munc13-4 and Rab27a together regulate a common secretory mechanism.

Importantly, the defects observed in azurophilic granule exocytosis of *Jinx* and *ashen* neutrophils were not due to a defect in the signaling mechanism activated downstream of Toll-like receptor 4-ligand recognition since mobilization of $\beta_2$ integrins in response to LPS was normal in Munc13-

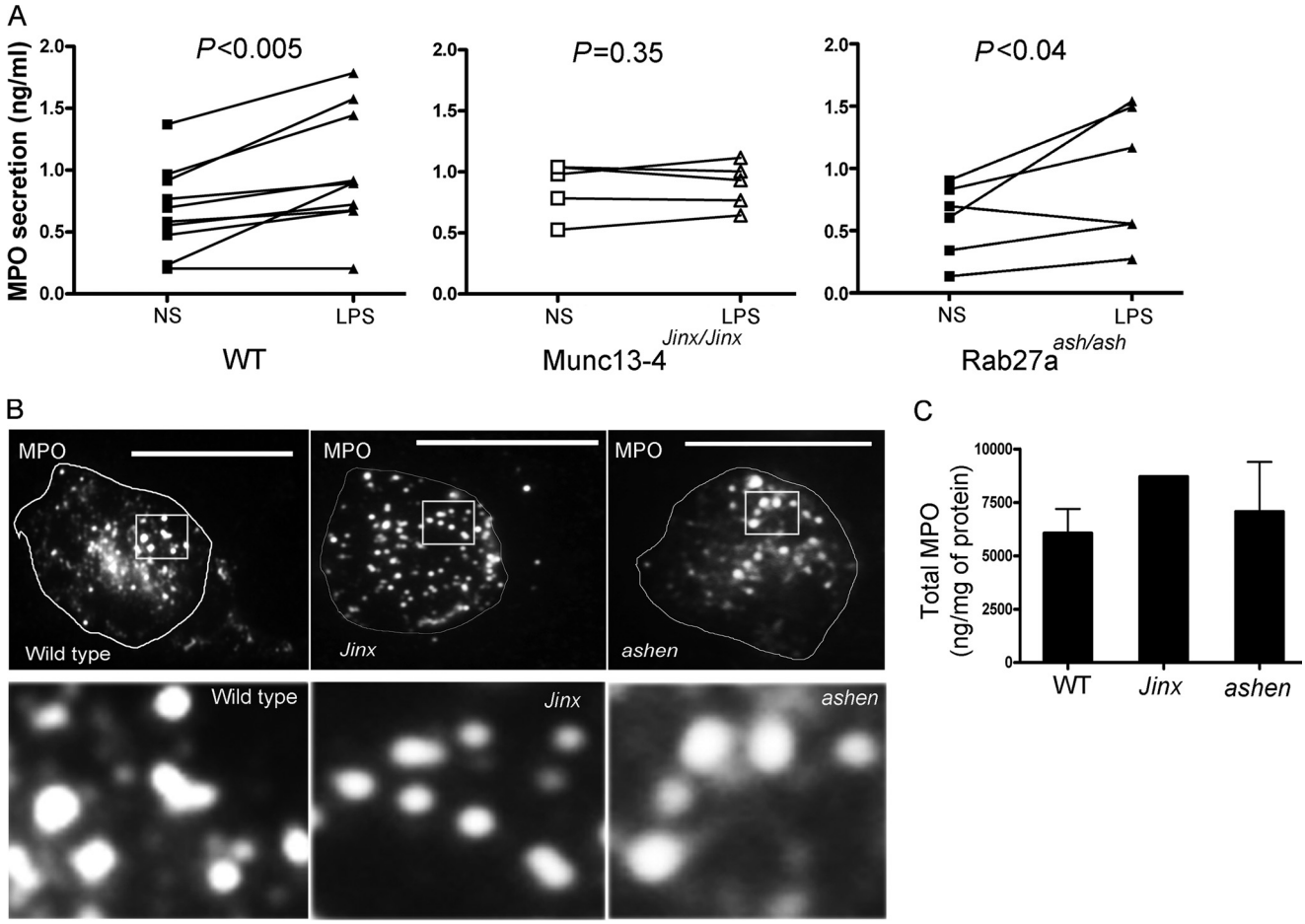


FIGURE 2. **Munc13-4 but not Rab27a controls the secretion of a small readily releasable pool of azurophilic granules.** *A*, each *symbol* corresponds to an independent sample from WT, Munc13-4-deficient (*Jinx*), or Rab27a-deficient (*ashen*) mice. Statistically significant differences were calculated using paired Student's *t* test. *B*, representative TIRFM images of neutrophils showing granular distribution of endogenous MPO. Magnifications of the areas selected in the *upper panels* are shown in the *lower panels*. *C*, total MPO in neutrophil cell lysates was measured by ELISA. *NS*, unstimulated.

$4^{Jinx/Jinx}$ and Rab27a$^{ash/ash}$ neutrophils (Fig. 1, *C* and *D*). In this way, mobilization of CD11b, which is stored in peroxidase-negative granules in neutrophils (23), proceeds independently of Munc13-4 or Rab27a expression and responds to both LPS activation and priming (Fig. 1*D*). CD11a, an adhesion molecule that is constitutively expressed in the plasma membrane of the neutrophil (23) and due to its differential response to stimuli is believed not to be stored in the same granules with CD11b (24), was slightly but significantly up-regulated in response to LPS treatment (Fig. 1*C*). This differs from previous studies showing lack of CD11a up-regulation in response to stimuli (24) but is in agreement with others showing increased CD11a expression after treatment with chemotactic peptides and chemokines (25), probably reflecting differences in antibodies affinities or different responses from neutrophils of different species. In any case, the up-regulation of $\beta_2$ integrins in response to LPS was similar in neutrophils from *Jinx*, *ashen*, and control mice further supporting that the defects observed in azurophilic granule exocytosis are not caused by intrinsic abnormalities of the signaling pathway initiated by TLR4 activation.

*Mobilization of Readily Releasable Vesicles Is a Munc13-4-dependent but Rab27a-independent Mechanism*—Although the secretory response of wild type neutrophils to LPS was relatively weak (Fig. 1, *A* and *B*), it was still significantly different from that observed in untreated neutrophils (Fig. 2*A*). This secretory response to LPS that represents the mobilization of a small (1.3 ± 0.7% of total mobilizable vesicles), readily releasable, pool of vesicles was null in neutrophils from Munc13-$4^{Jinx/Jinx}$ mice but present in Rab27a$^{ash/ash}$ neutrophils (Fig. 2*A*). Based on the data presented in Figs. 1 and 2, we suggest that Munc13-4 and Rab27a share a common mechanism in LPS-dependent priming of exocytosis but not in the LPS-induced mobilization of readily releasable vesicles, which appears to be a Munc13-4-dependent but Rab27a-independent process.

Furthermore, neutrophils from Munc13-$4^{Jinx/Jinx}$ and *Rab27a*$^{ash/ash}$ mice showed normal distribution of azurophilic granule cargo proteins (Fig. 2*B*) as well as normal levels of MPO expression (Fig. 2*C*) and cellular ultrastructure (3, 22), ruling out developmental defects and highlighting mechanistic defects in Munc13-4- and Rab27a-deficient neutrophils.

*LPS Increases Redistribution of Munc13-4 to Rab27a-associated Organelles at Plasma Membrane*—Previous studies presented evidence that Munc13-4 and Rab27a localized at distinct vesicular structures that mature along the exocytic pathway in cytotoxic T lymphocytes (16). In particular, Munc13-4 was suggested to be essential for the recruitment of endosomal recycling organelles to the Rab27a-associated late

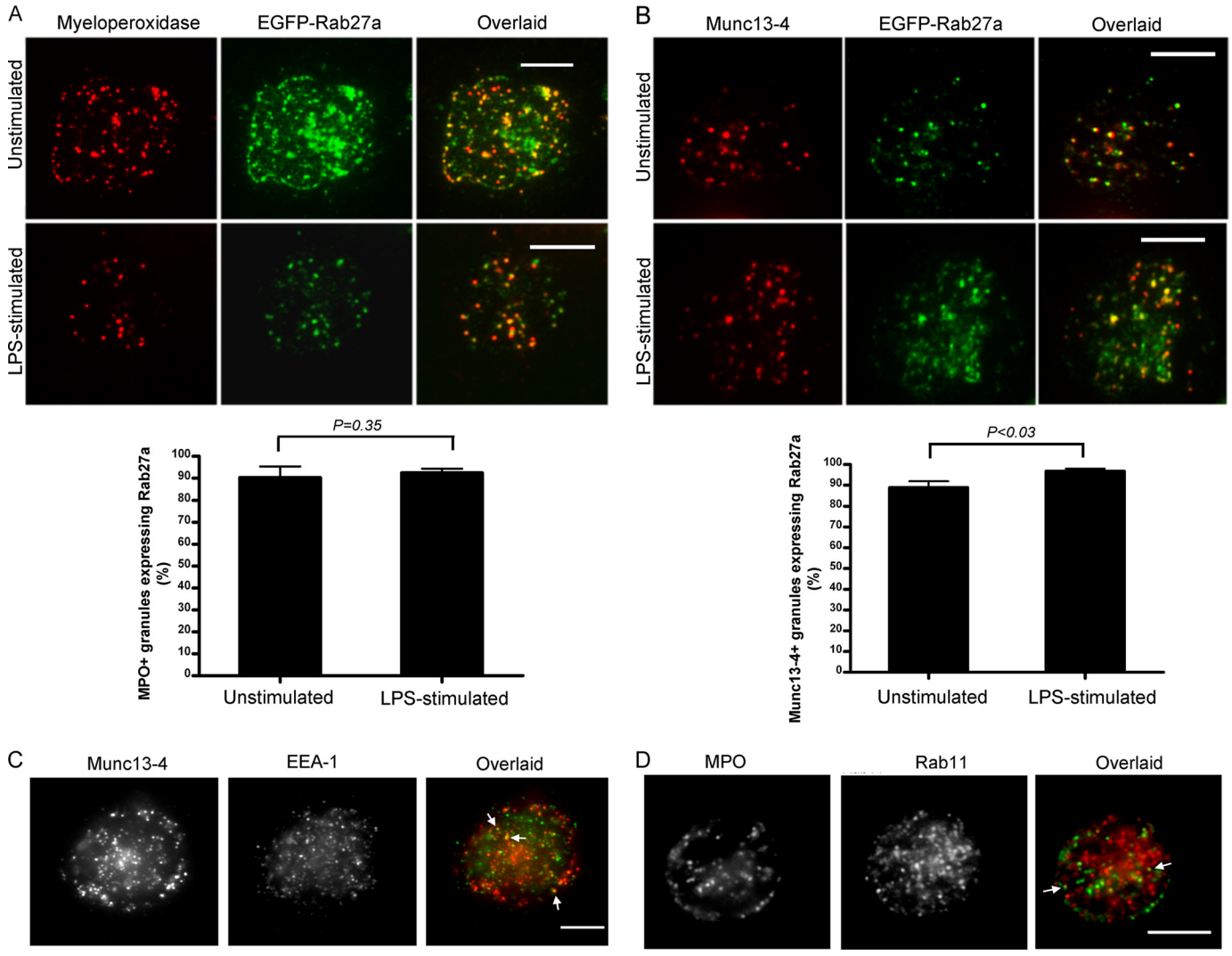


FIGURE 3. **Granule maturation in response to LPS at the exocytosis active site involves moderate Munc13-4 redistribution to Rab27a-expressing granules but not Rab27a redistribution to azurophilic granules.** The distribution of endogenous MPO (*A*) or Munc13-4 (*B*), and Rab27a was analyzed by TIRFM microscopy after immunostaining of LPS-treated or unstimulated cells. At least six cells from each condition were analyzed. Quantification of the distribution of the indicated proteins is shown in the *lower panels*. Results represent the mean ± S.E. *C* and *D*, control immunofluorescence experiments showing minimal colocalization (*arrows*) of Munc13-4 with the early endosome marker EEA-1 and MPO with the small GTPase Rab11 in unstimulated neutrophils. Similar results were observed in LPS-treated cells (supplemental Fig. S1).

endosomal compartments in cytotoxic T lymphocytes, a mechanism referred to as "granule maturation" (16). Whether this mechanism is present in other hematopoietic cells remains unclear. Furthermore, little is known about the possible maturation processes that may take place near the plasma membrane, subsequent to vesicular transport and prior to exocytosis. Here, to analyze a possible role of lipopolysaccharide stimulation in vesicle maturation, we studied the distribution of endogenously expressed secretory proteins on vesicles located in close proximity to the plasma membrane using a total internal reflection fluorescence microscopy approach. In Fig. 3*A*, we show that virtually all MPO-containing vesicles that are located in close proximity to the plasma membrane are associated with Rab27a-expressing structures in neutrophils. This clearly differs from that observed in vesicles that are not associated with the PM in which only a subpopulation of azurophilic granules containing MPO also expresses Rab27a (7). In principle, our results support the idea that only those azurophilic granules that express Rab27a would be able to engage in exocytosis. Next, we analyzed the effect of LPS stimulation on the distribution of Rab27a on plasma membrane-associated azurophilic granules. We show that LPS treatment does not significantly change the number of azurophilic granules that are associated with Rab27a near the plasma membrane, thus ruling out a possible role of Rab27a redistribution in LPS-dependent priming of exocytosis of azurophilic granules. In similar experiments, we analyzed the distribution of Munc13-4 related to that of Rab27a in vesicles located in the 100-nm range from the plasma membrane. Interestingly, we found that although most granules containing Munc13-4 distributed near the PM also express Rab27a (88.8 ± 3.16%, Fig. 3*B*), this colocalization parameter was significantly increased after LPS treatment (96.7 ± 1.64%), supporting the idea that a mechanism involving vesicle maturation may contribute, at least in part, to LPS-dependent priming of neutrophil exocytosis. Importantly, control

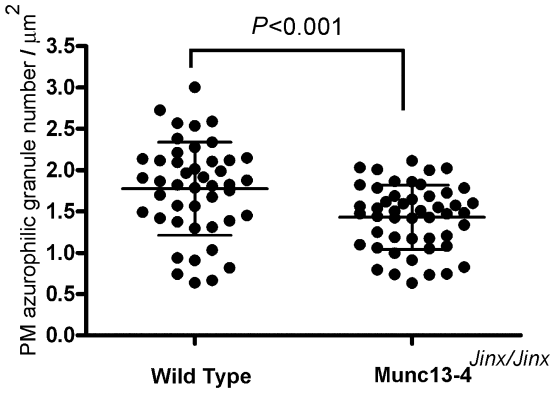


FIGURE 4. **Munc13-4-deficient neutrophils have a decreased number of azurophilic granules in proximity to the plasma membrane.** The quantitative analysis of the distribution of azurophilic granules in close proximity to the PM is shown. The distribution of endogenous MPO-containing granules in wild type and Munc13-4$^{Jinx/Jinx}$ neutrophils was determined by TIRFM. Representative images of each cell type are shown in Fig. 2. The number of azurophilic granules identified in the TIRFM zone (calibrated at <100 nm from the coverslip) per adherent membrane area unit for wild type or Munc13-4-deficient (*Jinx*) neutrophils is shown. *Bars* represent the mean ± S.D. Statistical analysis was performed using unpaired Student's *t* test. Each *symbol* represents an independent cell. 45–50 cells from three independent mice of each group were analyzed.

TIRFM experiments show lack or very little colocalization between MPO and the GTPase Rab11 and between Munc13-4 and the early endosome marker early endosomal antigen 1 (EEA-1) in proximity of the PM of untreated (Fig. 3, *C* and *D*) or LPS-treated (supplemental Fig. S1) cells, thus supporting the specificity of the staining for colocalized proteins.

*Quantitative Analysis of Azurophilic Granule Distribution in Munc13-*$^{Jinx/Jinx}$ *Neutrophils Revealed a Role for Munc13-4 in Azurophilic Granule Residency Near the Plasma Membrane*—Previous studies from our laboratory showed that Rab27a-deficient neutrophils have a decreased number of azurophilic granules in proximity to the plasma membrane and suggested that GTPases from the Rab27 family play a role in either vesicular transport to the plasma membrane or docking in neutrophils (22). Here, we show that virtually all MPO and Munc13-4-containing granules distributed at the plasma membrane also express Rab27a (Fig. 3) and that neutrophils deficient in Rab27a or Munc13-4 presented similar secretory defects (Fig. 1). To further analyze the relationship between Munc13-4 and Rab27a and to investigate whether Munc13-4 plays a significant role in azurophilic granule docking or residency in proximity to the plasma membrane, we next quantified the distribution of azurophilic granules in Munc13-4$^{Jinx/Jinx}$ neutrophils using TIRF microscopy. Using endogenous myeloperoxidase as the granule marker, we show that neutrophils from Munc13-4$^{Jinx/Jinx}$ mice have decreased numbers of azurophilic granules in the TIRFM zone (~100 nm from the PM) (Fig. 4), suggesting that Munc13-4 facilitates azurophilic vesicle trafficking toward the PM or mediates vesicle residency at the docking site before exocytosis. Based on the similar phenotypes observed in Munc13-4-null and Rab27a-deficient neutrophils, we suggest that they together regulate a vesicular transport step in exocytosis of secretory lysosomes in these cells.

*Munc13-4 Restricts Motility of Rab27a-expressing Vesicles to Facilitate Lipopolysaccharide-induced Priming of Exocytosis*—Highly dynamic events are known to take place in the plane of the plasma membrane and immediately before secretory granules fuse with the PM (18). The mechanisms that regulate these events are currently unknown and the participation of Rab27a or Munc13-4 in this process is unclear. In this study, we analyzed the priming effect of LPS on neutrophil exocytosis and dissected the dynamic processes that take place during the amplification of the secretory response. To this end, neutrophils from Tg$^{EGFP\text{-}Rab27a}$ and Tg$^{EGFP\text{-}Rab27a}$-Munc13-4$^{Jinx/Jinx}$ were stimulated with LPS and Rab27a-expressing vesicle dynamics were analyzed by TIRFM in primed cells (Fig. 5*A* and supplemental Movies 1–4). The quantitative analysis shows that Rab27a-expressing secretory organelles located near the plasma membrane and moving in the plane parallel to the plasma membrane undergo a significant decrease in speed after LPS treatment (Fig. 5*B*). In this way, the percentage of granules undergoing movement at a speed of 0.1 $\mu$m/s or above was significantly decreased after LPS treatment in wild type neutrophils (Fig. 5*B*). This correlated with a significant increase in the percentage of granules with restricted motility (average speed below 0.03 $\mu$m/sec) after treatment with LPS. Similarly, we observed a significant decrease in the number of highly motile granules (defined as those with track length of at least 0.5 $\mu$m with a speed equal or above 0.1 $\mu$m/s) after LPS treatment in Munc13-4-expressing cells (Fig. 5*C*). These data suggest that LPS treatment increases the number of tethered or docked granules at the PM, a process that could prepare secretory organelles for a subsequent step in exocytosis, *i.e.* fusion of the vesicle membrane to the PM. Next, to investigate the role of Munc13-4 in LPS-dependent vesicle docking, we analyzed EGFP-Rab27a-expressing vesicle dynamics in Munc13-4-deficient neutrophils. We found that in unstimulated cells lacking Munc13-4 neither the number of granules moving at high speed nor the total number of motile granules was significantly different from untreated wild type cells (Fig. 5, *B* and *C*). However, in response to LPS, Munc13-4-deficient cells failed to undergo a significant decrease in vesicle speed or motion, suggesting that Munc13-4 plays a fundamental role in LPS-dependent Rab27a-expressing vesicle priming and exocytosis by restricting granule motility at the PM. Interestingly, LPS-stimulated Munc13-4-deficient cells showed a significant increase in the number of granules with speed ranging between 0.04–0.05 $\mu$m/sec but not in granules with a speed range between 0 and 0.03 $\mu$m/sec (Fig. 5*B*), suggesting that the step regulating vesicle transition from slow movement to docking is regulated by Munc13-4. Importantly, the average speed of those granules that remain highly motile after LPS treatment was not significantly different from the speed of highly motile granule in untreated cells (Fig. 5*D*), indicating that LPS induces granule transition from a pool associated with a transport machinery to a pool of low motility granules associated with the PM rather than interfering with the actual transport system of highly motile granules to slow down vesicle movement.

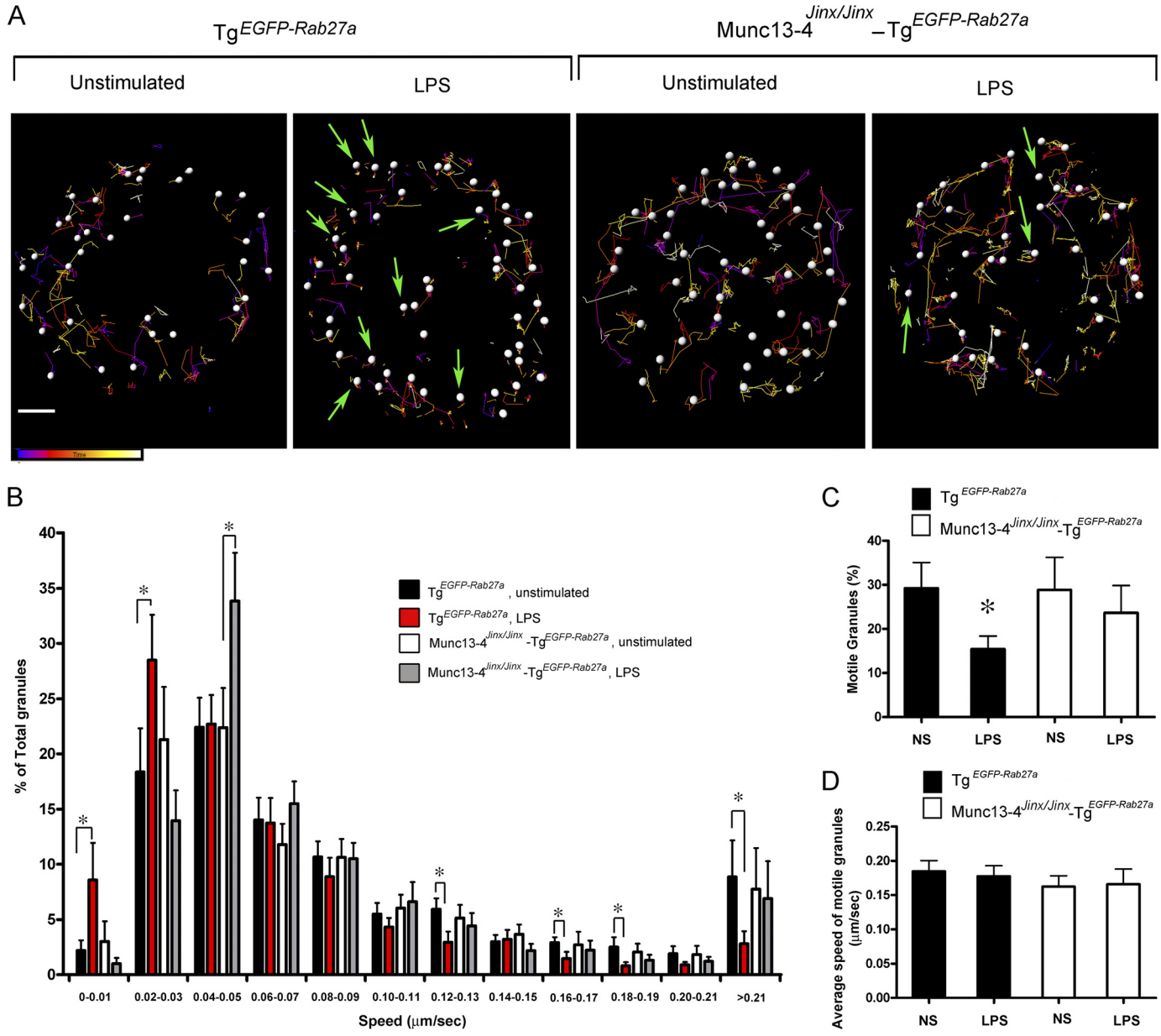


FIGURE 5. **LPS treatment induces motility restriction of Rab27a-expressing granules in a Munc13-4-dependent manner.** Kinetics of the distribution of Rab27a-expressing granules near the plasma membrane. Neutrophils from EGFP-Rab27a transgenic mice ($Tg^{EGFP\text{-}Rab27a}$) or Munc13-4 deficient EGFP-Rab27a transgenic mice (Munc13-$4^{Jinx/Jinx}$-$Tg^{EGFP\text{-}Rab27a}$) were isolated from peripheral blood and analyzed by TIRFM. Neutrophils were stimulated with LPS (100 ng/ml) for 2 h before analysis or left untreated. *A*, representative images of vesicular dynamic analysis of unstimulated or LPS-treated neutrophils. The dynamics of the labeled vesicles and the spatio-temporal displacement of Rab27a were followed for 2 min. Each *sphere* represents a vesicle. The tracks indicate the trajectory of the associated vesicles occurring during the analysis. *Increasing color* in a given track is indicative of time of appearance and residence in the TIRF zone. Tracks without a corresponding vesicle indicate that the vesicle appeared in the TIRF zone at a different frame from that shown. *Scale bar*, 2 $\mu$m. The dynamics of these vesicles during the length of the analysis can be observed in supplemental Movies 1–4, and the quantitative analysis is shown in the *lower panels* (*B–D*). Granules with decreased motility are indicated with *green arrows*. 12 to 23 different cells from three independent mice were analyzed for each condition in independent experiments. A total of 2368 vesicles (nonstimulated $Tg^{EGFP\text{-}Rab27a}$); 1493 vesicles (LPS, $Tg^{EGFP\text{-}Rab27a}$); 2157 vesicles (nonstimulated, Munc13-$4^{Jinx/Jinx}$-$Tg^{EGFP\text{-}Rab27a}$) and 1267 vesicles (LPS, Munc13-$4^{Jinx/Jinx}$-$Tg^{EGFP\text{-}Rab27a}$), which appeared in the TIRFM zone during the length of the study were included in the analysis. *B*, histograms of the speeds of Rab27a-containing granules from wild type and Munc13-4-deficient, LPS-treated or untreated neutrophils. Speeds for neutrophil granules were binned in 0.02-$\mu$m/s increments and plotted as a percentage of total granules for a given cell. Results are represented as mean ± S.E. *, $p < 0.05$. *C*, motile granules were defined as those with average speed > 0.1 $\mu$m/s and displacement > 0.5 $\mu$m. Results represent the mean ± S.E. The *asterisks* indicate a $p$ value <0.03 *versus* the unstimulated control (*NS*). *D*, no significant differences in the average speed of granules with speed >0.1 $\mu$m/s was detected for any of the groups evaluated.

*LPS Treatment Limits Displacement and Speed of Motion-restricted "Docked" Granules in a Munc13-4-dependent Manner*—Rather than being completely motionless, we observed that motion-restricted granules from wild type cells undergo significant movement that is characterized by local, apparently random displacement limited to a relatively small area parallel to the PM with an average diameter of ~0.5 $\mu$m (Fig. 6). This indicates that granules, which are putatively docked, are able to visit subdomains of the plasma membrane of a much more restricted area than undocked granules. Next, we further analyzed the effect of LPS on granule priming by measuring the dynamics of the subpopulation of motion-restricted granules

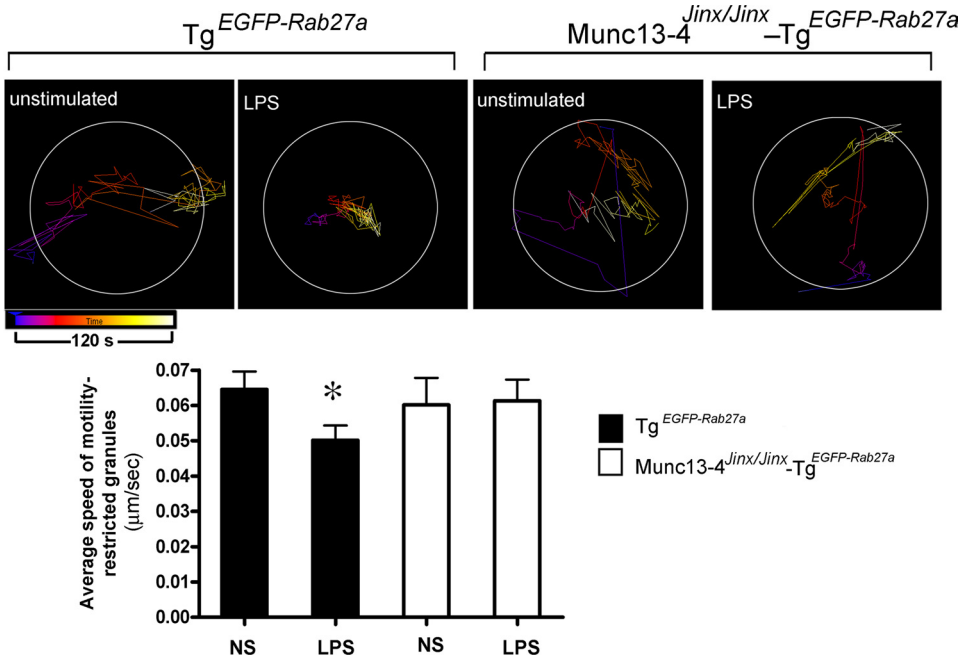


**FIGURE 6. LPS induces decrease of the speed and displacement of motion-restricted granules in a Munc13-4-dependent manner.** *Upper panels*, representative images showing kinetics of granules with displacement $< 0.5$ $\mu$m for each condition. Motility of granules with short displacement (those for which the distance between the coordinates at the beginning and the end of the analysis was $< 0.5$ $\mu$m) was significantly restricted after LPS treatment in wild type cells but not in Munc13-4-deficient neutrophils. Also, the average speed of motion-restricted granules was significantly decreased after LPS treatment in wild type cells but not in Munc13-4-deficient neutrophils (*lower panel*). The diameter of the circles depicted represents 0.5 $\mu$m. Results represent the mean ± S.E. The *asterisk* indicates a *p* value $<0.03$ *versus* the unstimulated control (*NS*, *black column*).

(displacement below 0.5 $\mu$m). In Fig. 6, we show that LPS induces a significant decrease in the average velocity and displacement of motion-restricted granules. Importantly, this effect was also dependent on Munc13-4 function as the LPS-dependent effect was abolished in neutrophils lacking Munc13-4.

## DISCUSSION

Neutrophil exocytosis plays an important role in extracellular bacterial killing and response to infection (2, 26), but uncontrolled release of the toxic content of azurophilic granules in response to LPS is potentially injurious to the host and contributes to the development of sepsis (27), highlighting the need of a tightly regulated mechanism of control. At the molecular level, both Rab27a and Munc13-4 have been involved in the regulation of exocytosis in hematopoietic cells, including neutrophils, a mechanism that is regulated not only spatially but also temporally. However, lack of dynamic studies have precluded a better understanding of the mechanism regulated by Rab27a and effectors during secretory lysosome exocytosis and whether Rab27a and Munc13-4 control discrete steps or the same steps in exocytosis is currently unclear. In this study, using neutrophils from Rab27a- and Munc13-4-deficient mice, we show that these secretory proteins coordinate a common step during vesicular priming in neutrophils. Furthermore, using neutrophils from a novel mouse model expressing EGFP-Rab27a at endogenous levels but lacking Munc13-4, we unraveled a novel mechanism of vesicular docking in which Munc13-4 restricts motility of Rab27a-expressing vesicles to facilitate lipopolysaccharide-induced priming of exocytosis.

Here, we show that deficiencies in either Rab27a or Munc13-4 led to similar impaired neutrophil secretory responses to bacteria-derived peptides in both primed and unprimed cells. However, Munc13-4 but not Rab27a was essential for the mobilization of a small, readily releasable pool of azurophilic granules. This suggests, for the first time, that neutrophils contain two populations of secretory azurophilic granules that differ in their tendency to undergo exocytosis, thus raising the question of whether they play different roles during neutrophil activation. Despite containing myeloperoxidase, it is not clear whether these vesicles share similar composition of cargo proteins, and additional studies will be necessary to further characterize these subpopulations of azurophilic granules. As for their secretory machinery, although Munc13-4 was originally described as a Rab27a-specific effector (10), Rab27a-independent functions have been proposed for Munc13-4 in other cells with secretory lysosomes (14, 15). A possible molecular mechanism regulating the secretion of readily releasable vesicles may involve Rab27b, a small GTPase that shares 72% homology with Rab27a at the amino acid level (28, 29), which is also expressed in neutrophils and whose deficiency leads to a mild defective secretory phenotype in these cells (22).

Our results suggest that putative redistribution of Munc13-4 between secretory organelles, a mechanism previously referred to as granule maturation (16), occurs in close proximity to the plasma membrane in LPS-treated neutrophils. This narrows the spatial distribution of at least some of the phenomena regulated by Munc13-4 to an area that is parallel and immediately adjacent to the plasma membrane,

hereupon denominated the "active, exocytic space" or "active zone." We therefore chose TIRFM as the technical approach to study the role of Munc13-4 in the regulation of the spatiotemporal distribution of secretory organelles in LPS-induced priming. Using this approach, we found that in unstimulated wild type cells virtually all granules that contain myeloperoxidase and are in close proximity to the PM also express Rab27a (Fig. 3). Because only a low percentage of internally distributed azurophilic granules express Rab27a (7), these data suggested that Rab27a is important for azurophilic granule residency in the active, exocytic space. This is further confirmed by previous studies showing that Rab27a-deficient neutrophils have a decreased number of azurophilic granules in the active, exocytic zone (22). Furthermore, because LPS treatment did not affect the distribution of Rab27a related to the localization of MPO in the active exocytic space, we ruled out a possible role of Rab27a relocalization in the mechanism of LPS-induced priming of azurophilic granule exocytosis.

Our experiments show that Munc13-4-deficient neutrophils present impaired azurophilic granule residency at the active exocytic space. A similar defect in the distribution of azurophilic granules at the plasma membrane was observed in Rab27a-deficient unstimulated neutrophils, whereas Rab27b- deficient cells presented a less significant defect (22). To better understand whether the similar phenotypes observed in *ashen* and *Jinx* neutrophils correlate with a common role in azurophilic granule exocytosis for Rab27a and Munc13-4, we next analyzed the distribution of these secretory proteins at the active exocytic space in unstimulated and LPS-treated cells. We found that 89% of all Munc13-4-expressing granules that are located near the PM also contain Rab27a (Fig. 3). In our studies, we also observed that after LPS treatment, Munc13-4 undergoes a significant redistribution increasing the number of granules containing both Rab27a and Munc13-4 that are present in the active zone to almost 96%. This strongly supports a common role for these secretory proteins in azurophilic granule exocytosis in response to LPS activation. Although these results suggest a possible role of vesicle maturation in LPS-induced priming similar to the mechanism previously described in cytotoxic T lymphocytes (16), it is highly unlikely that a ~7% increase in colocalization could independently explain the almost 50% increase in exocytosis observed after LPS-induced priming. Notwithstanding, our data strongly support a common role for Munc13-4 and Rab27a in the regulation of lysosome-related organelles. This differs from previous studies in platelets and NK cells, which suggested that Rab27a and Munc13-4 regulate discrete rather than common steps in exocytosis (14, 15). However, those conclusions were drawn based on static observations and the authors addressed the need for further analysis to determine how the interaction between Munc13-4 and Rab27 is required for membrane trafficking (15).

To better understand a phenomenon that is dynamic in nature, we next utilized neutrophils from a novel mouse model expressing EGFP-Rab27a at endogenous levels but lacking Munc13-4. In the EGFP-Rab27a transgenic mouse, EGFP-Rab27a expression is regulated under the endogenous *Rab27a* promoter, so that the level of expression and distribution of the transgenic protein faithfully mimics that of endogenous Rab27a (21). Furthermore, expression analysis from our laboratory shows that EGFP-Rab27a is expressed at a similar level to the endogenous Rab27a in neutrophils where it localizes at secretory organelles. (Fig. 3 and supplemental Fig. S2). Also, previous work by Tolmachova *et al.* (21) showed that crossing the EGFP-transgenic mice with *ashen* mice rescue the *ashen* phenotype, further supporting that the EGFP-Rab27a transgene is both appropriately expressed and functional. Thus, although in some transgenic models high protein expression may nonspecifically affect cellular function, it is unlikely that EGFP-Rab27a expression affects vesicle dynamics or obscures functional effects of Munc13-4 loss in this model.

Using TIRFM in conjunction with quantitative spatiotemporal analysis of vesicle trafficking in live cells, we demonstrate that LPS-dependent priming involves a dramatic reduction in Rab27a-expressing vesicle speed and displacement. Because the average speed of those granules that remain as fast-moving granules after LPS treatment was not different from the speed of fast-moving granules in untreated cells, our results suggest that LPS induces the transition of vesicles from a high motility to a low motility state rather than interfering with the transport mechanism of highly motile vesicles. Thus, LPS treatment seemed to favor the docking of Rab27a-expressing vesicles at the PM. As this mechanism was abolished in the absence of Munc13-4, our results also indicate that Munc13-4 is an essential component of the docking machinery of Rab27a-expressing organelles.

It is still unclear how LPS favors the docking process. LPS-dependent stimulation of neutrophils induces both changes in the phosphorylation state of secretory proteins (6) as well as variations in the composition of microdomains at the PM (1); therefore, either changes of the phosphorylation state of Munc13-4 or changes in the phospholipidic composition of docking microdomains at the PM could favor motility restriction of secretory organelles. In any case, the observation that motion-restricted organelles are still able to visit areas in close proximity to the docking site, suggests that LPS induces a "loose docking" mechanism and highlights the need of dynamic approaches to characterize the function of secretory proteins. We speculate that this loose docking will increase the probability of a given vesicle localizing at a fusion site when a second stimuli triggers exocytosis. Supporting this hypothesis, previous studies showed that secretory vesicles that undergo rapid movement immediately after stimulation have a higher tendency to undergo exocytosis (18).

Altogether, our data strongly support the concept that LPS treatment induces vesicle tethering or docking by decreasing the speed of exocytosis-competent Rab27a-expressing vesicles that move in a plane parallel to the PM. Our data also support a role for Munc13-4 as an essential regulator of vesicle priming and exocytosis during LPS-induced neutrophil stimulation and propose that Munc13-4 plays a central role in the

regulation of Rab27a-expressing vesicle exocytosis by controlling the dynamic events that takes place during LPS-induced vesicular priming.

*Acknowledgments—We thank Dr. Miguel Seabra for contributing the EGFP-Rab27a transgenic mouse and Dr. Bruce Beutler for contributing the Munc13-4$^{Jinx/Jinx}$ mouse. We also thank Dr. Sandy Schmid for access to the TIRF microscope.*

## REFERENCES

1. Brzezinska, A. A., Johnson, J. L., Munafo, D. B., Ellis, B. A., and Catz, S. D. (2009) *Immunology* **127,** 386–397
2. Standish, A. J., and Weiser, J. N. (2009) *J. Immunol.* **183,** 2602–2609
3. Brzezinska, A. A., Johnson, J. L., Munafo, D. B., Crozat, K., Beutler, B., Kiosses, W. B., Ellis, B. A., and Catz, S. D. (2008) *Traffic* **9,** 2151–2164
4. Condliffe, A. M., Kitchen, E., and Chilvers, E. R. (1998) *Clin. Sci.* **94,** 461–471
5. Shahin, R. D., Engberg, I., Hagberg, L., and Svanborg Edén, C. (1987) *J. Immunol.* **138,** 3475–3480
6. Ward, R. A., Nakamura, M., and McLeish, K. R. (2000) *J. Biol. Chem.* **275,** 36713–36719
7. Munafó, D. B., Johnson, J. L., Ellis, B. A., Rutschmann, S., Beutler, B., and Catz, S. D. (2007) *Biochem. J.* **402,** 229–239
8. Griscelli, C., Durandy, A., Guy-Grand, D., Daguillard, F., Herzog, C., and Prunieras, M. (1978) *Am. J. Med.* **65,** 691–702
9. Feldmann, J., Callebaut, I., Raposo, G., Certain, S., Bacq, D., Dumont, C., Lambert, N., Ouachée-Chardin, M., Chedeville, G., Tamary, H., Minard-Colin, V., Vilmer, E., Blanche, S., Le Deist, F., Fischer, A., and de Saint Basile, G. (2003) *Cell* **115,** 461–473
10. Neeft, M., Wieffer, M., de Jong, A. S., Negroiu, G., Metz, C. H., van Loon, A., Griffith, J., Krijgsveld, J., Wulffraat, N., Koch, H., Heck, A. J., Brose, N., Kleijmeer, M., and van der Sluijs, P. (2005) *Mol. Biol. Cell* **16,** 731–741
11. Shirakawa, R., Higashi, T., Tabuchi, A., Yoshioka, A., Nishioka, H., Fukuda, M., Kita, T., and Horiuchi, H. (2004) *J. Biol. Chem.* **279,** 10730–10737
12. Fukuda, M. (2005) *J. Biochem.* **137,** 9–16
13. Stinchcombe, J. C., Barral, D. C., Mules, E. H., Booth, S., Hume, A. N., Machesky, L. M., Seabra, M. C., and Griffiths, G. M. (2001) *J. Cell Biol.* **152,** 825–834
14. Wood, S. M., Meeths, M., Chiang, S. C., Bechensteen, A. G., Boelens, J. J., Heilmann, C., Horiuchi, H., Rosthøj, S., Rutynowska, O., Winiarski, J., Stow, J. L., Nordenskjöld, M., Henter, J. I., Ljunggren, H. G., and Bryceson, Y. T. (2009) *Blood* **114,** 4117–4127
15. Ren, Q., Wimmer, C., Chicka, M. C., Ye, S., Ren, Y., Hughson, F. M., and Whiteheart, S. W. (2010) *Blood* **116,** 869–877
16. Ménager, M. M., Ménasché, G., Romao, M., Knapnougel, P., Ho, C. H., Garfa, M., Raposo, G., Feldmann, J., Fischer, A., and de Saint Basile, G. (2007) *Nat. Immunol.* **8,** 257–267
17. Pivot-Pajot, C., Varoqueaux, F., de Saint Basile, G., and Bourgoin, S. G. (2008) *J. Immunol.* **180,** 6786–6797
18. Degtyar, V. E., Allersma, M. W., Axelrod, D., and Holz, R. W. (2007) *Proc. Natl. Acad. Sci. U.S.A.* **104,** 15929–15934
19. Crozat, K., Hoebe, K., Ugolini, S., Hong, N. A., Janssen, E., Rutschmann, S., Mudd, S., Sovath, S., Vivier, E., and Beutler, B. (2007) *J. Exp. Med.* **204,** 853–863
20. Wilson, S. M., Yip, R., Swing, D. A., O'Sullivan, T. N., Zhang, Y., Novak, E. K., Swank, R. T., Russell, L. B., Copeland, N. G., and Jenkins, N. A. (2000) *Proc. Natl. Acad. Sci. U.S.A.* **97,** 7933–7938
21. Tolmachova, T., Anders, R., Stinchcombe, J., Bossi, G., Griffiths, G. M., Huxley, C., and Seabra, M. C. (2004) *Mol. Biol. Cell* **15,** 332–344
22. Johnson, J. L., Brzezinska, A. A., Tolmachova, T., Munafo, D. B., Ellis, B. A., Seabra, M. C., Hong, H., and Catz, S. D. (2010) *Traffic* **11,** 533–547
23. Bainton, D. F., Miller, L. J., Kishimoto, T. K., and Springer, T. A. (1987) *J. Exp. Med.* **166,** 1641–1653
24. Kuijpers, T. W., Tool, A. T., van der Schoot, C. E., Ginsel, L. A., Onderwater, J. J., Roos, D., and Verhoeven, A. J. (1991) *Blood* **78,** 1105–1111
25. Mortier, A., Loos, T., Gouwy, M., Ronsse, I., Van Damme, J., and Proost, P. (2010) *J. Biol. Chem.* **285,** 29750–29759
26. Nathan, C. (2006) *Nat. Rev. Immunol.* **6,** 173–182
27. Brovkovych, V., Gao, X. P., Ong, E., Brovkovych, S., Brennan, M. L., Su, X., Hazen, S. L., Malik, A. B., and Skidgel, R. A. (2008) *Am. J. Physiol. Lung Cell Mol. Physiol.* **295,** L96–103
28. Barral, D. C., Ramalho, J. S., Anders, R., Hume, A. N., Knapton, H. J., Tolmachova, T., Collinson, L. M., Goulding, D., Authi, K. S., and Seabra, M. C. (2002) *J. Clin. Invest.* **110,** 247–257
29. Gomi, H., Mori, K., Itohara, S., and Izumi, T. (2007) *Mol. Biol. Cell* **18,** 4377–4386